NEW METHOD OF EUTECTIC SILICON MODIFICATION IN CAST Al–Si ALLOYS

A. M. Samuel and F. H. Samuel
Université du Québec à Chicoutimi, Chicoutimi, QC, Canada

H. W. Doty
General Motors, Materials Engineering, Pontiac, MI, USA

S. Valtierra
Nemak, S.A, Garza Garcia, NL, Mexico

DOI 10.1007/s40962-016-0089-4

Abstract

The aim of the present work was to investigate various means of obtaining a fine eutectic silicon structure in A356.2 alloy and therefore improve the alloy mechanical properties. The effects of solidification rate, Sr modification and melt thermal treatment (MTT) on the silicon particle characteristics of A356.2 (Al–7 %Si–0.4 %Mg) alloy were studied. The particle characteristics measured were the average particle area, average particle length, average particle roundness and average particle aspect ratio, using image analysis and optical microscopy. The results showed that Sr modification-, superheat- and Sr modification-MTT (SrMTT)-processed castings provide fine eutectic Si particles, the SrMTT process giving the best modification results. Both size and morphology of the eutectic silicon particles are affected by the modification process used. The Sr-grain-refined, Sr-melt superheat and SrMTT castings show well-modified fibrous Si particles, whereas the MTT casting exhibits Si particles that, although refined to a certain extent, still retain their acicular morphology. Solidification rate affects the eutectic Si particle size in that a higher solidification rate produces finer Si particles. However, within the range of solidification rates provided by the end-chill mold used in this work, the solidification rate does not affect the morphology of the Si particles.

Keywords: *melt thermal treatment, melt superheat, Sr modification, eutectic Si particle characteristics*

Introduction

The Al–Si–Mg alloy system has excellent casting characteristics, weldability, pressure tightness and corrosion resistance. With heat treatment, Al–Si–Mg alloys can provide a wide range of physical and mechanical properties. Such alloys are commonly used in automobile components.[1]

Among Al–Si–Mg alloys, A356.2 is a commercially popular alloy, known for its excellent mechanical properties and high strength-to-weight ratio. The use of a heat treatment consisting of, for example, a solution heat treatment at 540 °C, followed by quenching and natural or artificial aging, allows for the formation of interdendritic non-equilibrium precipitates of Mg_2Si and changes in the Si particle characteristics.[1,2] The A356.2 alloy contains 0.3–0.45 % Mg which can induce age hardening through the precipitation of Mg_2Si; the higher the Mg content, the more the age hardening that can be achieved. During solidification of A356, as the melt temperature drops to 577.6 °C (widely accepted as the Al–Si eutectic temperature),[3] the Al–Si eutectic reaction takes place. This reaction occurs at 577.6 °C, at a Si level of ~12 %.

$$\text{A356 alloy liquid} \rightarrow Al_{eut} + Si_{eut}$$

As can be seen, the liquid alloy is completely transformed to nearly pure Si and Al in solid solution. The solid solution of Al can contain up to 1.5 wt% Si at the eutectic temperature. However, the solubility of silicon in aluminum decreases with temperature, e.g., to 0.05 wt% at 300 °C.[4] The Al–Si eutectic nucleates on the primary aluminum dendrites and grows into the interdendritic regions during the reaction. From the Al–Si binary phase

diagram, it can be estimated that A356 (Al–7 %Si–0.4 %) alloy contains approximately 50 % Al–Si eutectic.

The Si particle characteristics, especially the morphology, also influence the mechanical properties, where a change from an acicular to a fibrous morphology improves the properties, in particular, ductility. In this regard, molten metal processing (melt treatment) and casting techniques as well as the type of heat treatment applied are the factors by which the form and size of the Si particles can be controlled.[1] Several elements are known to cause eutectic Si modification. Group IA and Group IIA elements of the Periodic Table, i.e, rare earth elements (e.g, La, Ce), As, Sb, Se and Cd, have all been reported to exert a modification effect.[5] However, only sodium (Na), strontium (Sr) and antimony (Sb) have ever been used commercially. Among them, Sb, due to its toxic effects, is not used in North America. Due to its low boiling point, the 'fading' or poor retention of Na in the melt once added, leaves Sr as the modifier of choice in present-day foundry operations.

Melt thermal treatment (MTT) appears to be a promising alternative to chemical modification in that it can reduce some of the latter's negative effects such as increased porosity. Analysis of MTT-processed Al–Si alloy castings show that the resulting microstructure is significantly refined, leading to a considerable increase in the tensile strength-to-elongation ratio.[6]

The present research work was undertaken to investigate various means of obtaining a fine eutectic Si in the as-cast microstructure of the A356.2 alloy via the effects of solidification rate, Sr modification, super heating, and melt thermal treatment.

Experimental Procedure

The A356.2 casting alloy was received in the form of 12.5 kg ingots. Table 1 lists the chemical composition of the as-received ingots. The A356.2 ingots were cut into smaller pieces, cleaned, dried and melted in a 7-kg capacity SiC crucible, using an electrical resistance furnace. The melting temperature was kept at 750 ± 5 °C.

During the preparation of the castings corresponding to various melt treatments and conditions, 6-kg charges of A356.2 alloy were melted in each case. The melts, per 6-kg charge of metal, were grain-refined, using 55 g of Al–5 %Ti–1 %B master alloy. Degassing was carried out using pure dry argon, injected into the melt by means of a graphite rotary degassing impeller. The degassing time/speed was kept constant at 30 min/150 rpm. Figure 1a shows the reduced pressure test (RPT) images before and after degassing. It should be mentioned here that the humidity was about 27 %.

For the preparation of the Sr-modified (SrM) castings, the melt was modified using a Al–10 %Sr master alloy after degassing, where 12 g of the master alloy was added (to the 6 kg charge) to provide a Sr level of 200 ppm. The melt was stirred carefully and held for ~20 min to ensure proper dissolution of Sr into the melt, followed by another 10 min of degassing prior to pouring. Table 2 summarizes the details corresponding to all of the prepared castings.

For the preparation of castings using superheated (SH) melts, the melt temperature was increased to 900 °C, with the melt being held at this temperature for 20 min and then poured into the mold. Castings were prepared using a rectangular end-chilled mold. The four walls of the mold are made of refractory material, while the bottom consists of a water-chilled copper base, to provide directional solidification. This type of mold is designed to provide a range of solidification rates along the height of the casting above the chill end.

The mold was preheated at 225 °C for at least 2–3 h to remove all moisture. The molten metal was poured into the mold through ceramic foam filter disks fitted into the riser to avoid oxides and inclusions from entering the mold. The water (circulating in the copper chill) was turned on as soon as the liquid metal had filled the mold to 3 cm. Such an arrangement produced ingot blocks with solidification rates that decreased with increasing distance from the chill end, giving microstructures that exhibited secondary dendrite arm spacings (SDAS) from 15 to 85 μm along the height of the cast block.

For the preparation of castings using the MTT process, a 6-kg charge of A356.2 alloy was melted at 750 °C, grain-refined and degassed using the same procedures already described. Following this, 4 kg of the melt was transferred to the other furnace, already preheated to 750 °C. The temperature of the first furnace was then lowered to 600 °C, while that of the second was increased to 900 °C. The corresponding low-temperature melt (LTM) and high-temperature melt (HTM) were held at their respective temperatures for 20 min, followed by 15 min of degassing. The HTM melt was then poured into the LTM melt, and the

Table 1. Chemical Composition of as-Received A356.2 Ingot (wt%)

Alloy	Si	Mg	Fe	Cu	Mn	Zn	Ti	Pb	Al
A356.2	6.78	0.33	0.11	0.02	0.04	0.04	0.08	0.03	Bal.

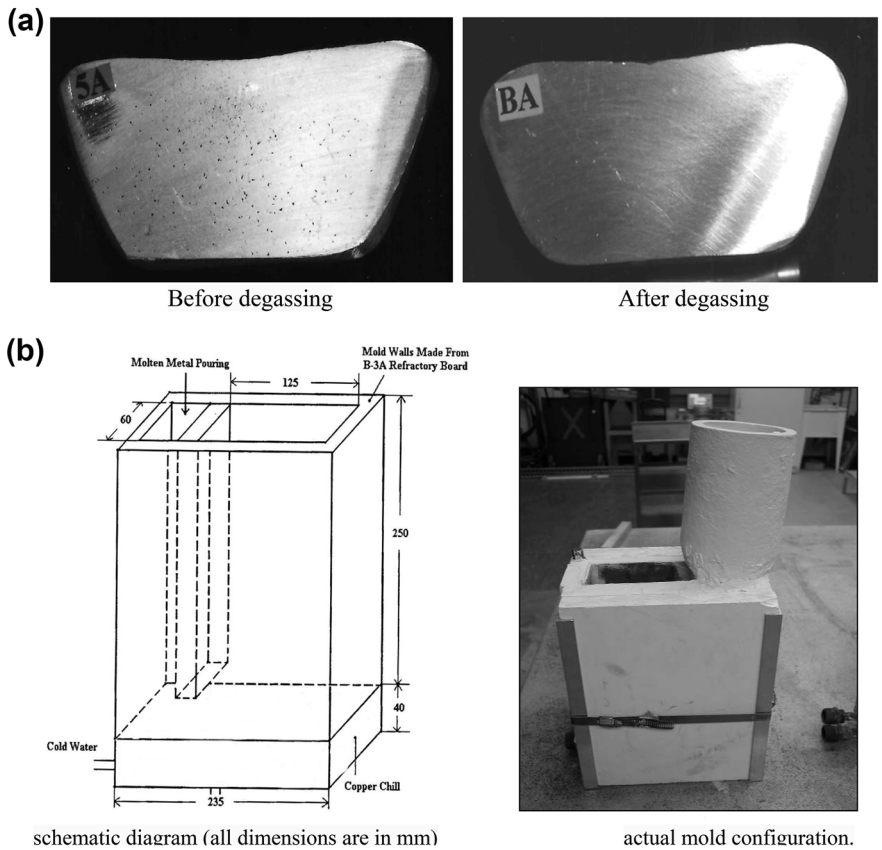

Figure 1. (a) RPT tests of samples before and after degassing. (b) The end-chilled mold used to prepare the castings in the present study. (c) Grain size along the solidification axis from grain-refined melt—see Table 4.

Table 2. Details of the Various A356.2 End-Chill Castings Prepared for the Present Work

Casting type	Melt Condition/treatment	Charge	Additions to charge	Melt/pouring temperature (°C)	No. of castings prepared
NM	As-received (non-modified) + grain refined	6 kg	55 g Al–5 % Ti–1 % B	750	10
SrM	Grain refined	6 kg	55 g Al–5 % Ti–1 % B	750	10
	+ Sr modified		12 g Al–10 % Sr		
SH	Grain refined + superheated (900 °C)	6 kg	55 g Al–5 % Ti–1 % B	900	6
MTT	MTT process treated	6 kg	55 g Al–5 % Ti–1 % B	670	6
	Non-modified + grain refined				
	LTM (600 °C)	(2 kg)			
	HTM (900 °C)	(4 kg)			
SrMTT	MTT process treated	6 kg		670	6
	Grain refined + Sr modified		55 g Al–5 % Ti–1 % B		
			3 g Al–10 % Sr		
	LTM (600 °C)	(2 kg)			
	HTM (900 °C)	(4 kg)			

mixture stirred carefully, followed by pouring into the end-chilled mold.

For the preparation of Sr-modified (and grain-refined) castings using the MTT process (SrMTT), the same procedure was followed, except that the initial 6-kg melt was modified using 10 g of Al-10 % Sr master alloy to give a Sr level of 100 ppm, followed by degassing for another 10–15 min. Following this, 4 kg of the modified melt was transferred to the other furnace and the same procedures followed of preparing the LTM and HTM melts, mixing them and then pouring the melt into the end-chilled mold. Table 3 lists the chemical analysis of all alloys used in the present work.

The end-chill castings that were prepared according to ASTM E8-04 standards, corresponding to the various melt treatments and processes were sectioned to obtain blanks and, subsequently, samples for metallography and tensile testing. Figure 1b shows the end-chill setup used for the production of all castings studied in the present investigation, whereas Figure 1c illustrates the increase in the grain size along the solidification axis in the grain-refined alloys.

The tensile test bars were prepared from specimen blanks sectioned from three locations in the casting block, such that the centrelines of the blanks corresponded to 10-, 50- and 100-mm levels above the chill end, as shown in Figure 2. The tensile test bars were pulled to fracture at room temperature at a strain rate of 4×10^{-4} s^{-1}, using a Servohydraulic MTS mechanical testing machine. A strain gauge extensometer (with a 50.8 mm range) was attached to the test bar to measure percentage elongation as the load was applied. The data were analyzed using the TestWorks 4 software designed for tensile testing. The tensile properties, namely yield stress (YS) at a 0.2 % offset strain, ultimate tensile strength (UTS) and fracture elongation (%El), were derived from the data acquisition and data treatment systems of the software. The tensile properties of each alloy condition were represented by the average %El, YS and UTS values which were calculated over the values obtained from the five tensile test bars assigned to that condition.

Three specimen blanks were sectioned from each of the prepared castings, at heights of 10, 50 and 100 mm from the chill end, and corresponding to average SDAS of 37, 62 and 78 μm, respectively as shown in Table 4.

The SDAS values were determined by measuring the corresponding metallography samples using an optical microscope-image analyzer system. At least 40 measurements were taken for each sample, and the average value taken to represent the SDAS value for the corresponding level. A quantitative evaluation of the eutectic Si particle characteristics was carried out using image analysis. From these measurements, the average value and standard deviation were obtained in each case.

Results and Discussion

Silicon Particles Characterization

The optical micrographs taken from the various A356.2 alloy casting types are presented in this section. For simplicity, the five casting types studied will be referred to by their casting codes as shown in Table 3. Figure 3 displays the dendrite shape and size as-cast A356.2 alloy samples corresponding to level #1 and level #3. Figures 4, 5, 6, 7 and 8 show the eutectic Si particle characteristics displayed by the A356.2 alloy castings corresponding to the five

Table 3. Chemical Compositions of Various Types of Melts

Casting type	Casting no.	Si%	Mg%	Sr%	Ti%	Al%
NM	1	5.99	0.3219	<0.0000	0.1762	Bal.
	2	6.99	0.3849	0.0002	0.1694	Bal.
	3	6.58	0.3225	<0.0000	0.1601	Bal.
	4	6.54	0.3575	0.0001	0.1690	Bal.
	5	6.39	0.3571	0.0005	0.1826	Bal.
	6	6.00	0.3445	<0.0000	0.1709	Bal.
SrM	1	6.17	0.3039	0.0220	0.1353	Bal.
	2	6.26	0.3027	0.0204	0.1505	Bal.
	3	6.51	0.3069	0.0213	0.1684	Bal.
	4	6.60	0.2194	0.0202	0.1532	Bal.
	5	6.05	0.2396	0.0204	0.1500	Bal.
	6	6.33	0.2367	0.0203	0.1474	Bal.
SH	1	6.44	0.3237	0.0007	0.145	Bal.
	2	6.17	0.2839	0.0002	0.1273	Bal.
	3	6.05	0.3214	0.0005	0.1583	Bal.
	4	6.25	0.2998	0.0002	0.1358	Bal.
	5	6.63	0.3172	0.0004	0.1440	Bal.
	6	6.47	0.3282	0.0002	0.1401	Bal.
MTT	1	6.23	0.3085	0.0001	0.1435	Bal.
	2	6.03	0.3281	0.0002	0.1560	Bal.
	3	6.15	0.3177	0.0001	0.1345	Bal.
	4	5.89	0.3244	0.0002	0.1614	Bal.
	5	6.35	0.3130	0.0001	0.1406	Bal.
	6	7.66	0.2471	0.0012	0.1391	Bal.
SrMTT*	1	7.10	0.2962	0.0096	0.1531	Bal.
	2	7.12	0.3214	0.0118	0.1878	Bal.
	3	6.64	0.2992	0.0170	0.1401	Bal.
	4	7.04	0.3246	0.0161	0.1361	Bal.
	5	6.98	0.3069	0.0153	0.1260	Bal.
	6	6.91	0.3255	0.0126	0.1209	Bal.

* 100 ppm Sr (and not 200 ppm Sr) was used for the SrMTT melt to determine whether in using the MTT process, a lesser amount of Sr would suffice to obtain a well-modified eutectic structure

casting types. Each figure displays the microstructures obtained at levels 1, 2 and 3 of each casting.

As can be seen from Figure 4, the non-modified (NM) casting displays the typical acicular Si particles. Some amount of refinement due to solidification rate is observed in Figure 4a, compared to Figure 4b, c. In effect, the dendrite arm spacings of levels 2 and 3 are not that far apart, and hence, their microstructures would be more similar than different, particularly when compared to that of level 1, with a dendrite arm spacing almost half that of the others.

Tolui and Hellawell[7] and Hogan and Song[8] have reported that the Si interparticle spacing decreases with increase in solidification rate and vice versa. This is evidenced to some extent in Figure 4. With the introduction of 200 ppm Sr to the melt, the eutectic Si particles are completely transformed from long, acicular plates to well-modified fibrous particles. The very fine particle size results in a significant increase in the Si particle density. The observation of a well-modified eutectic structure in A356.2 alloys with Sr addition is well reported.[9,10]

In Figure 5, while the eutectic Si regions are well modified, a certain number of unmodified or partially modified Si particles are always observed close to the α-Al dendrites. This phenomenon is a result of the distribution of Si concentration within the α-Al dendrites. The areas close to the dendrites contain higher Si concentrations, requiring more strontium to become fully modified. However, due to the high solidification rate produced by the end-chill mold,

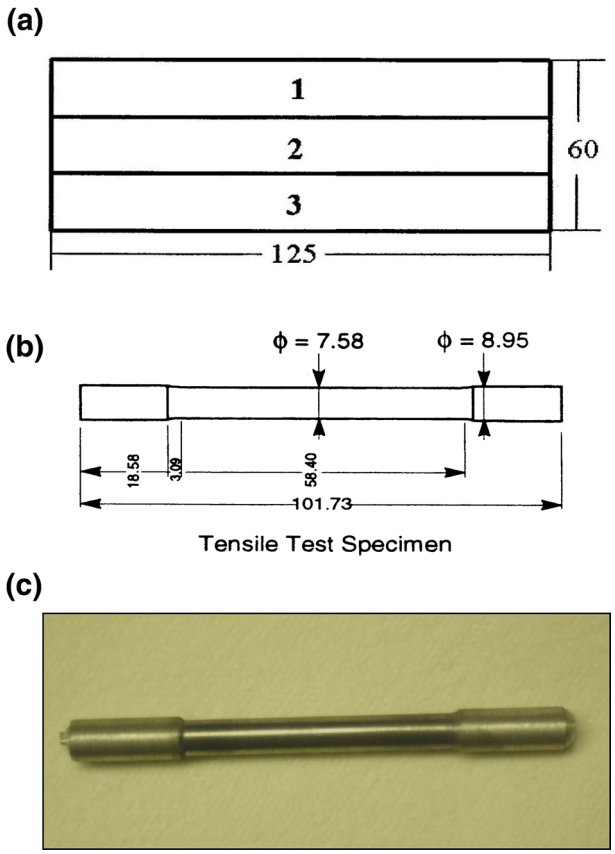

Figure 2. (a) Blank sectioning scheme for preparing tensile test specimens; (b) tensile test specimen dimensions (in mm); (c) actual tensile test specimen.

Table 4. SDAS Values Obtained at Various Levels of the End-Chill Casting

Level #	Distance from the chill end (mm)	SDAS (μm)
1	10	37
2	50	62
3	100	78

there is less time for the strontium to be distributed to these areas and thus there is not enough strontium available to fully modify the eutectic Si particles, leaving them partially modified or unmodified.

Figure 6 shows that superheating of the melt has a remarkable refining effect on the eutectic Si in A356.2 alloy. This effect can be attributed to the dissolution of atom clusters present in the melt at the superheat temperature. According to Pople and Sidorov,[11] if the superheat temperature is high enough for the atom clusters to dissolve fully in the melt, the solidification rate should have no effect on the eutectic Si particle characteristics in the microstructure. However, by comparing Figure 6a–c, it can be seen that the size of the eutectic Si particles increases somewhat as the solidification rate decreases, so it can be concluded that the 900 °C melt superheat temperature used in the present study is not high enough to achieve the same results. Therefore, in the present case, the microstructure of the eutectic Si particles is determined by both the superheat temperature and the solidification rate.

Figures 7 and 8 compare the effects of MTT on the microstructures of castings obtained from unmodified and Sr-modified A356.2 alloy melts, respectively. Although the eutectic Si particles are refined in the MTT-processed casting of the unmodified alloy, they still retain their acicular morphology. This observation was also reported by Wang et al.[13] A combination of Sr modification and the MTT process results in very fine eutectic Si regions, where the acicular, larger-sized Si particles that were observed at the edges of the α-Al dendrites in Figure 5 (for the Sr-modified alloy) appear to have been minimized considerably in the SrMTT casting (Figure 8).

In this regard, it should be mentioned that, in the MTT casting obtained from the non-modified A356.2 alloy, the refining (or modifying) effect was not homogeneous over the sample surface. As Figure 9 shows, the eutectic Si particles are a mix of refined and unrefined Si particles. This micrograph was taken from the MTT casting—level 1 sample. This irregularity in modification may be caused by the inhomogeneous transfer of thermal energy when the LTM and HTM melts are mixed. On account of this, atom clusters that are not broken into smaller nuclei will eventually result in the formation of larger Si particles upon solidification.

As previously mentioned, there appears to be very little literature that reports on the MTT process in the context of the modification of Al–Si alloys.[12] The present study extended the work of Wang et al.[13] to investigate the combined effect of Sr addition and the MTT process on the modification effect in the A356.2 alloy by modifying the alloy melt with 100 ppm Sr before subjecting it to the melt thermal treatment process. As Figure 8 shows, the combination of Sr modification and MTT process produces the best results as far as obtaining a well-modified eutectic is concerned. The uniformity of the eutectic Si particle size throughout the eutectic regions is remarkable. Compared to the 200 ppm SrM case, hardly any large Si particles are observed at the periphery of the α-Al dendrites.

It should be mentioned here that, for the SrMTT casting, only 100 ppm Sr was used, to determine whether a lesser amount of Sr than that usually employed for obtaining a well-modified eutectic structure in Al–Si alloys would suffice to obtain the same level of modification after the MTT process was carried out. A quantification of the eutectic Si particle characteristics using image analysis showed that the SrMTT casting samples provided the smallest Si particle sizes, followed by the SrM and then the SH casting samples. The level of modification observed in

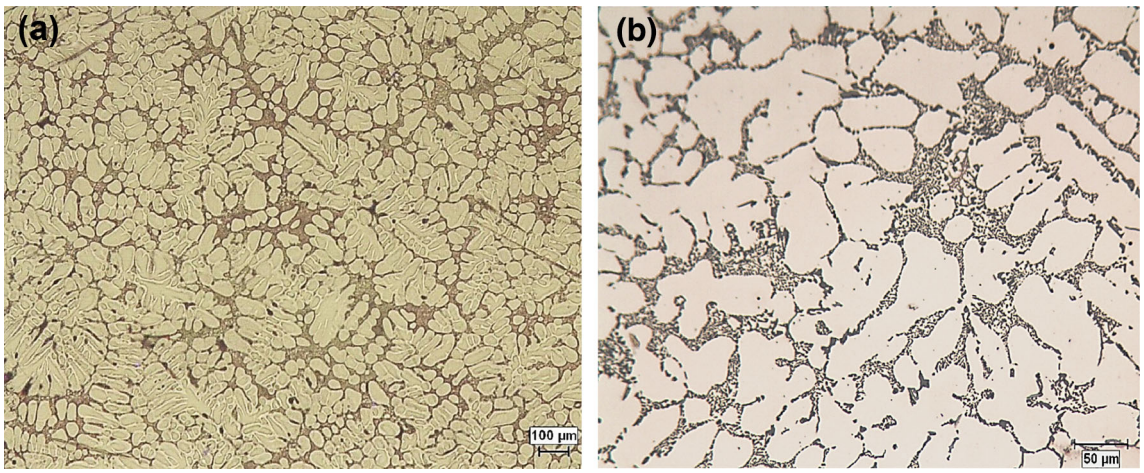

Figure 3. Optical microstructures of as-cast A356.2 alloy samples corresponding to: (a) level #1, (b) level #3.

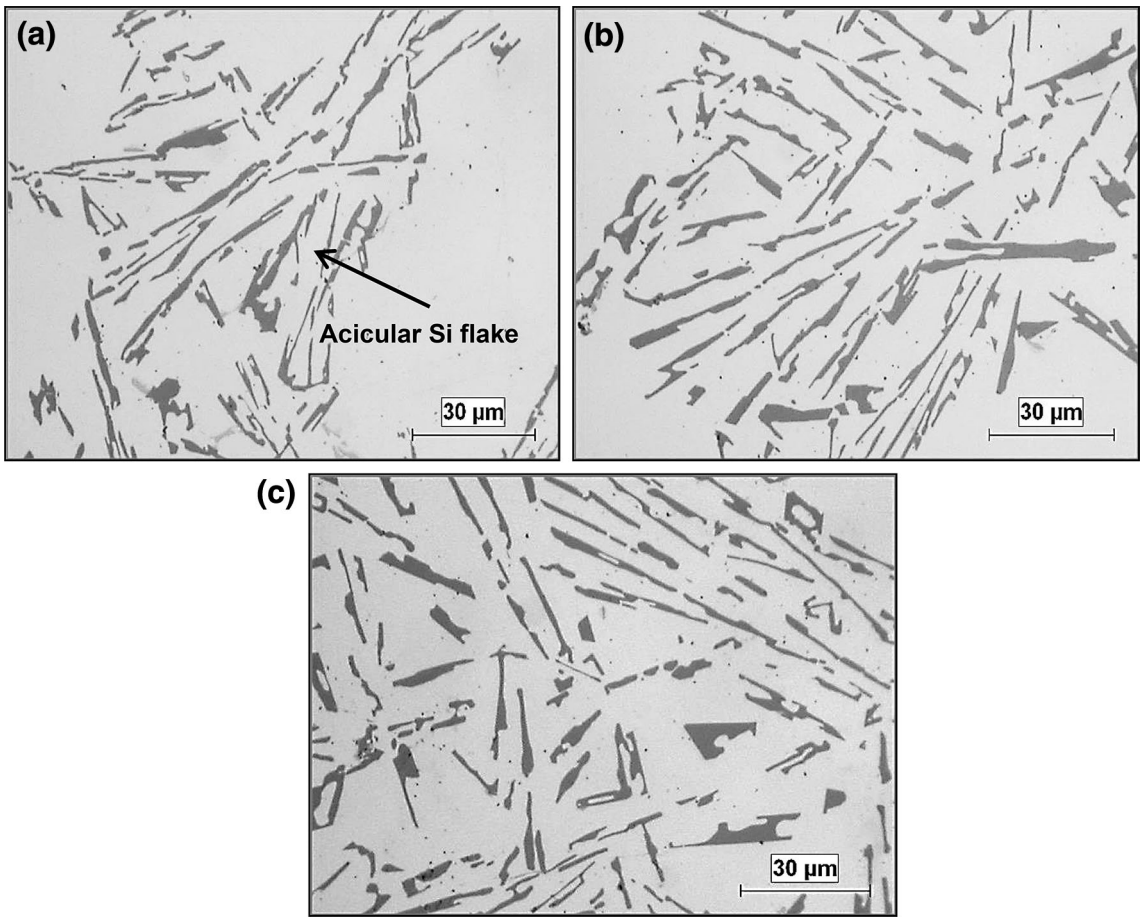

Figure 4. Optical micrographs showing the eutectic Si particle characteristics observed in as-cast samples of the NM (non-modified) A356.2 alloy casting: (a) level 1, SDAS 37 µm; (b) level 2, SDAS 62 µm; (c) level 3, SDAS 78 µm.

the different A356.2 alloy castings corresponding to the NM, SrM, 900 °C SH-, MTT-processed and SrMTT-processed castings is compared in Figure 10 for samples obtained from levels 1 and 3 of each casting, corresponding to SDAS values of 37 and 78 µm, respectively.

As can be seen, well-modified fibrous Si particles are produced with SrM, SH and SrMTT processes, the latter producing the finest particles, while the use of the MTT process alone is seen to only refine the Si particles but not change their acicular morphology. The effect of

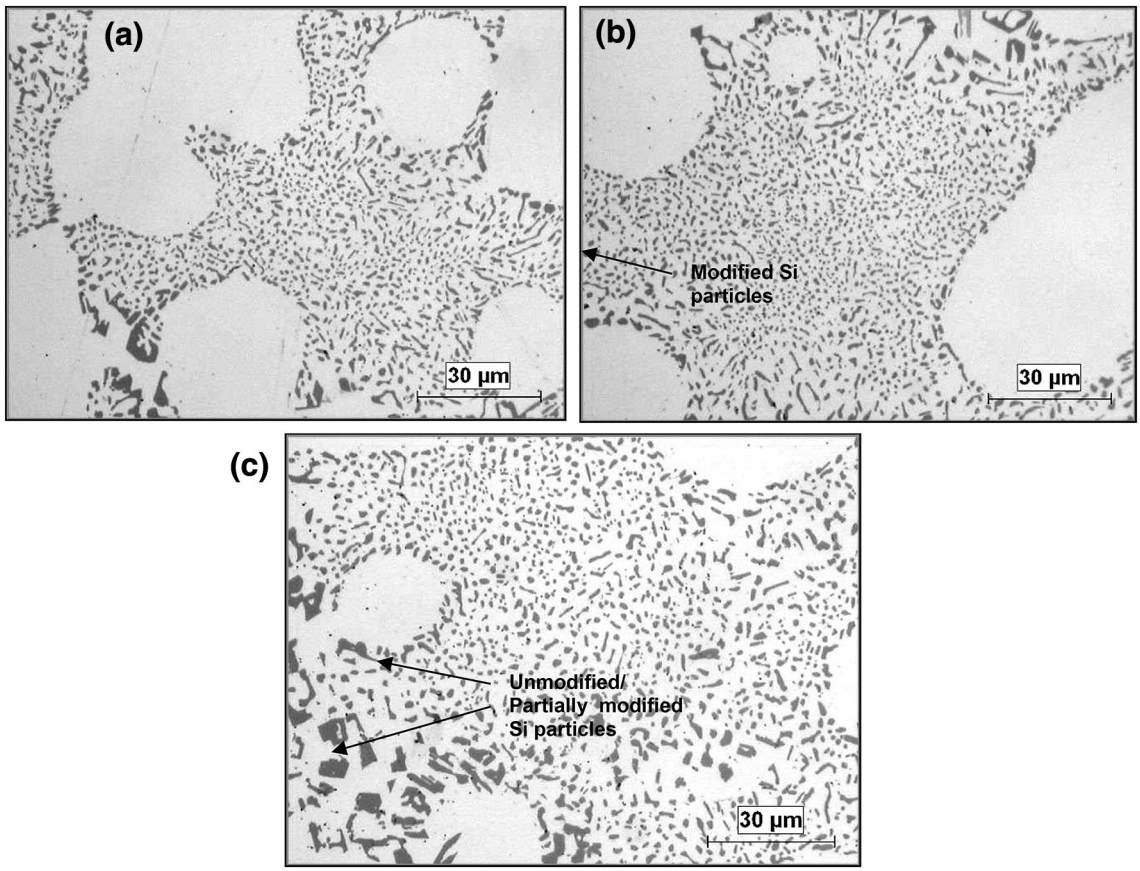

Figure 5. Optical micrographs showing the eutectic Si particle characteristics observed in as-cast samples of the SrM (200 ppm Sr-modified) A356.2 alloy casting: (a) level 1, SDAS 37 µm; (b) level 2, SDAS 62 µm; (c) level 3, SDAS 78 µm.

solidification rate is apparent for the MTT-processed samples (Figure 10g, h), and also evident to some extent in the NM, SrM and SH samples. The extremely fine Si particles in the case of the SrMTT casting render it difficult to distinguish the effect of solidification rate when comparing Figure 10i, j.

The effect of solidification rate on the Si particle characteristics in Al–Si alloys has been investigated by many researchers.[11–14] In the present study, the A356.2 alloy melts subjected to different modification methods were cast into end-chilled molds that provided a range of solidification rates in the same casting, along the height of the casting block. Three solidification rates were selected for study, at heights or levels of 10, 50 and 100 mm above the chill end and corresponding to SDAS values of 37, 62 and 78 µm, respectively. As the A356.2 alloy melts were modified before being cast, in examining the effect of solidification rate, the effects of the modification method used in each case would also be incorporated automatically.

Table 5 summarizes the results of the eutectic Si particle characteristics obtained for different samples in the as-cast condition. It can be seen that the solidification rate has a moderate to significant influence on the Si particle size in that the particle size increases as the solidification rate is decreased. The moderate effect is observed in the case of the non-modified alloy casting, where a gradual increase in the average Si particle area and length values are observed from level 1 to level 3. In comparison, the other four (modified) castings show a significant influence of the solidification rate, although this may not be that evident in the case of the SrMTT casting samples, compared to the MTT casting samples, on account of the very fine particle sizes obtained in the former. Similar results were reported by Mancheva et al.[14] who observed that the average Si particle area in AlSi7Mg castings improved from 0.9 to 0.4 μm^2 when the solidification rate was increased from 14.8 to 72.4 K/s.

While solidification rate affects the Si particle size, Figure 11 shows that the shape of the Si particles is not affected by the change in solidification rate. Both the average roundness and average aspect ratio values (and their standard deviations) remain more or less the same from one level to the next. This is to be expected, since these parameters relate to the morphology, rather than the size, of the Si particles, with roundness values close to 100 and an aspect ratio of 1.0 representing completely spherical particles. As can be seen, the acicular particles of the non-

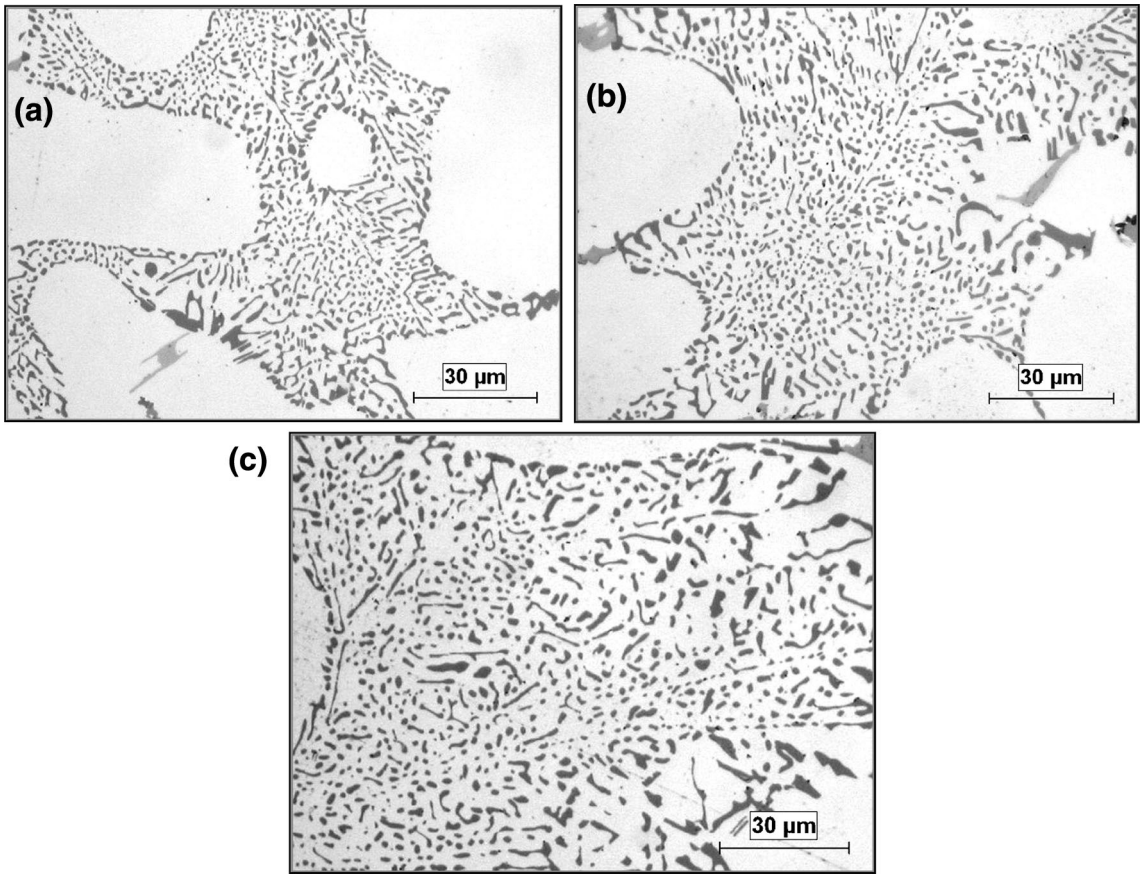

Figure 6. Optical micrographs showing the eutectic Si particle characteristics observed in as-cast samples of the SH (superheated) A356.2 alloy casting: (a) level 1, SDAS 37 µm; (b) level 2, SDAS 62 µm; (c) level 3, SDAS 78 µm.

modified alloy display low roundness values (<50 %) and high aspect ratios (2.6–3.3), whereas the SrM, SH and SrMTT castings have much higher roundness values (75–77 %) and comparatively lower aspect ratios (~1.8). The standard deviations obtained for these two parameters are also approximately similar for the SrM, SH and SrMTT castings (roundness value ~20 and aspect ratio ~0.7, respectively), indicating that these parameters are influenced by the modification process rather than the solidification rate.

In contrast to the modified castings discussed above, the MTT casting samples exhibit roundness and aspect ratio values that are comparable to, but somewhat lower than, those obtained for the non-modified alloys, indicating that the Si particles, although refined, still retain their acicular morphology. Also, the standard deviations observed for these two parameters for the MTT and NM casting samples are higher (~28 and ~1.35–1.7, respectively), compared to those noted for the SrM, SH and SrMTT castings.

Similar results corresponding to the NM and SrM castings in the present work were obtained by Paray and Gruzleski[15] in their studies on non-modified and Sr-modified A356 alloys. Their experimental results showed that for A356 alloy castings, drawn from a permanent mold, the average Si particle area was refined from 3.81 μm^2 in the non-modified alloy casting to 0.24 μm^2 in the 200 ppm Sr-modified alloy casting, and the average aspect ratio improved from 2.17 to 1.74.

With respect to the average and standard deviation values, listed in Table 5, it must be noted that, due to the wide range of Si particle sizes observed, it is expected that the standard deviation will be of the order of or higher than the average value. The particle size distribution plotted by the image analyzer system provides a range of Si particle sizes and the corresponding particle counts. It is found that the maximum particle count generally corresponds to the particle size range which includes or lies close to the average value calculated by the system. In other words, the average values *do* reflect the overall modification effect obtained from casting type to casting type.

The results of Table 5 are presented in Figures 10, 11, 12 and 13 in the form of histograms, which facilitate distinguishing the effect of solidification rate (or dendrite arm spacing), and that of the modification process on the Si particle characteristics. In general, the Si particle area and length of the MTT casting appear to be the most sensitive to the solidification rate, followed by the NM and SH

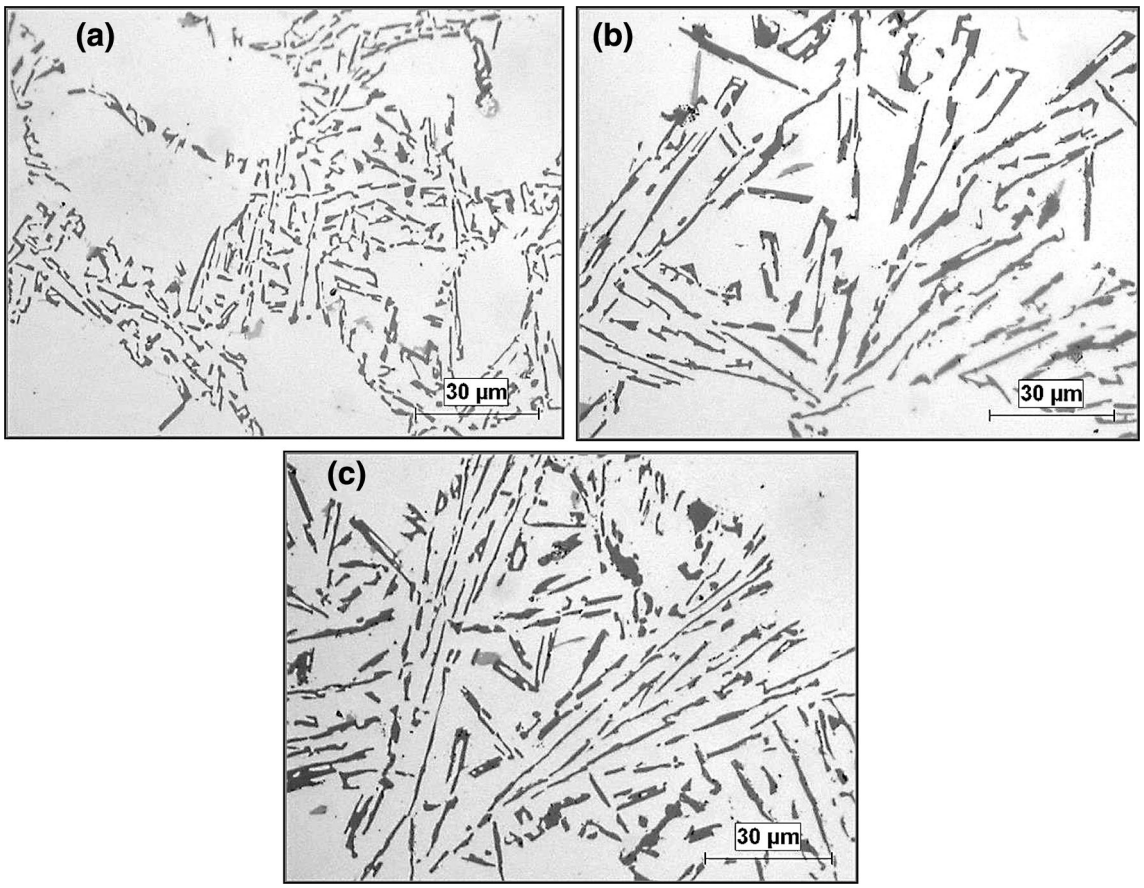

Figure 7. Optical micrographs showing the eutectic Si particle characteristics observed in as-cast samples of the MTT-processed A356.2 alloy casting: (a) level 1, SDAS 37 µm; (b) level 2, SDAS 62 µm; (c) level 3, SDAS 78 µm.

castings (Figures 11, 12). In the SrM casting, an improvement due to solidification rate is evidenced mainly at the solidification rate corresponding to the lowest SDAS (37 µm). The particle size remains constant at SDAS levels of 62 µm and above.

Compared to all these casting types, the SrMTT casting shows the best results in that not only the Si particle sizes are the smallest among all castings; however, these values remain approximately constant over the range of solidification rates studied. This has a great significance from an application point of view. Often, cast parts contain sections of varying thickness, and in such cases, the use of a SrMTT-processed Al–Si alloy melt in casting would ensure a relatively uniform eutectic Si particle size throughout the casting and, therefore, guarantee its overall properties.

With respect to the roundness parameter, the best results are obtained with the SrMTT casting which displays consistently high roundness values, with a very small influence due to solidification rate. The aspect ratios, however, are similar to those obtained for the SH and SrM castings. The moderate amount of refinement in the Si particle morphology in the MTT casting compared to the NM casting can also be observed from Figures 13 and 14.

The various modification methods applied to A356.2 alloy in the present work were used to determine which would produce a well-modified, fibrous eutectic structure, for example, those that reduced the Si particle size and aspect ratio to a minimum and increased the roundness to a maximum. Theoretically, spherical particles would have a roundness value of ~100 % and an aspect ratio of 1.

To compare the efficiencies of the different modification methods, the Si particle characteristics obtained for the SrM, SH, MTT and SrMTT casting samples were compared with those obtained for the NM casting in terms of the percentage *decrease* in the area and length parameters, the percentage *increase* in the roundness and the percentage *decrease* in the aspect ratio, as shown in Tables 6 and 7. The values in the parentheses in the row for the NM casting in both tables represent the actual values obtained for each parameter at the corresponding level. Those listed in the other rows provide the percentage changes in the four parameters (area, length, roundness and aspect ratio) observed in the other casting samples calculated in terms of the NM values in parentheses. The actual values are given in Table 5.

In their study of the effect of Sr modification in A356.2 alloy, Paray and Gruzleski[15] found that strontium affects

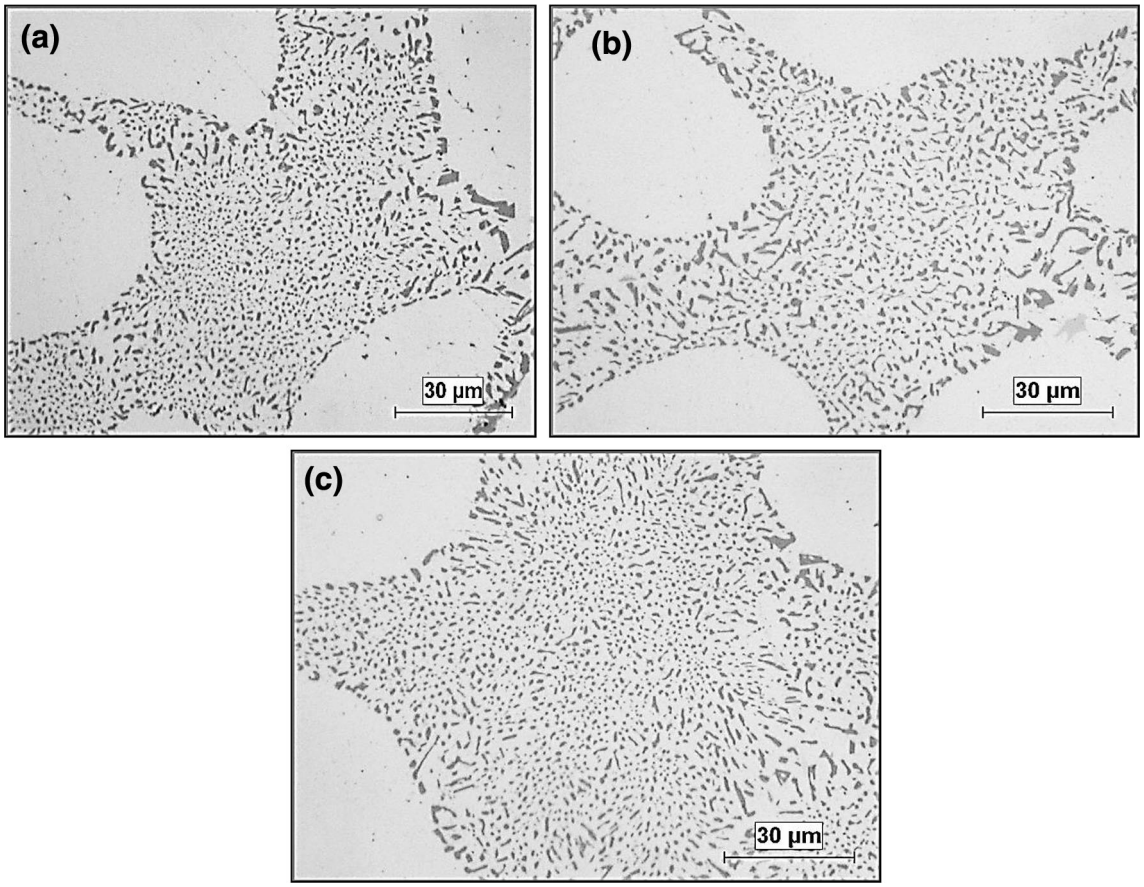

Figure 8. Optical micrographs showing the eutectic Si particle characteristics observed in as-cast samples of the SrMTT (100 ppm Sr-modified + MTT processed) A356.2 alloy casting: (a) level 1, SDAS 37 µm; (b) level 2, SDAS 62 µm; (c) level 3, SDAS 78 µm.

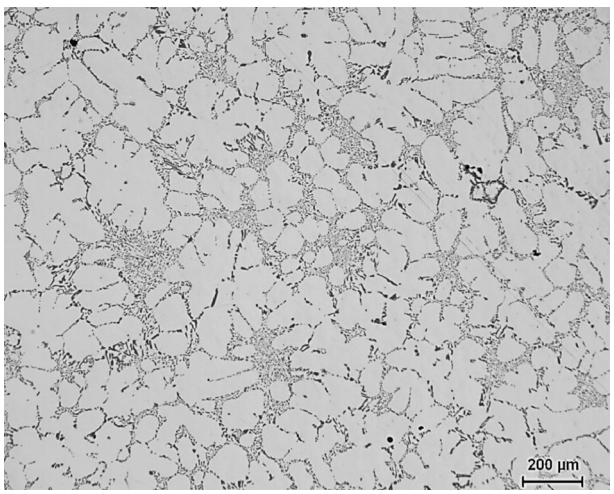

Figure 9. Optical micrograph corresponding to the MTT casting—level 1 sample, showing mixed refined eutectic Si regions.

not only the size and morphology of the eutectic Si particles, but also the particle size and morphology distribution. Their conclusions, which correspond to the NM and SrM castings in the present work, can also be extended to the SH, MTT and SrMTT castings, as well, where the standard deviation obtained for each parameter measured can be used to estimate the structural uniformity of the eutectic Si particles in A356.2 alloy. The smaller the standard deviation, the more homogeneous the Si particle size and morphology distribution: in other words, the higher the degree of modification achieved.

Tensile Properties and Fractography

The as-cast tensile properties of the various A356 alloy castings were determined, and the results were then plotted in Figures 15, 16, 17 and 18, where the term DAS, used interchangeably with SDAS, actually refers to the secondary dendrite arm spacing. According to Shivkumar et al.,[16] yield strength is mainly determined by the Mg content and the aging condition rather than the eutectic Si particle characteristics, or solidification rate in terms of secondary dendrite arm spacing. This observation is also corroborated by the experimental results obtained in the development of the current work.

As shown in Figure 16, under the same solidification rate, various modification methods produce a wide range of Si particles characteristics and hence the variation in the yield

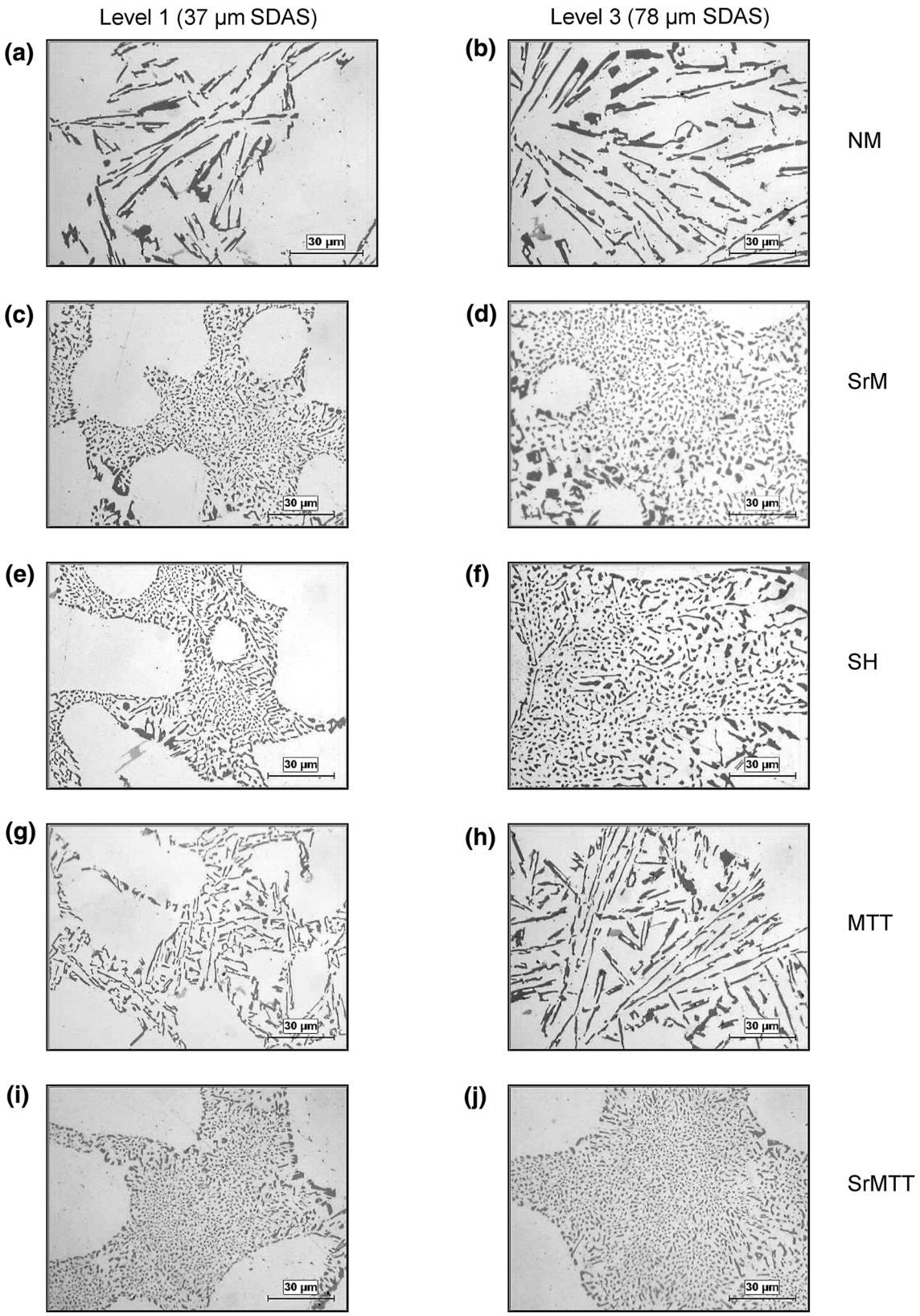

Figure 10. Comparison of modification in different A356.2 alloy samples obtained from: (a, b) NM, (c, d) SrM, (e, f) SH, (g, h) MTT and (i, j) SrMTT castings in the as-cast condition, and corresponding to levels 1 and 3 in each case.

Table 5. Eutectic Si Particle Characteristics of Different Casting Samples Obtained in the as-Cast Condition

Casting type	Area (μm²)						Length (μm)					
	Level 1 (SDAS 37 μm)		Level 2 (SDAS 62 μm)		Level 3 (SDAS 78 μm)		Level 1 (SDAS 37 μm)		Level 2 (SDAS 62 μm)		Level 3 (SDAS 78 μm)	
	Avg.	SD	Avg.	SD	Avg.	SD	Avg.	SD	Avg.	SD	Avg.	SD
NM	25.33	28.46	26.32	29.11	27.32	30.09	11.96	11.39	13.57	12.85	14.62	13.93
SrM	1.16	1.94	2.82	4.09	3.08	4.26	1.57	1.36	2.36	1.91	2.48	2.03
SH	1.62	3.37	2.8	4.45	4.4	6.2	1.94	2.04	2.62	2.54	3.29	2.96
MTT	2.94	4.56	5.04	8.48	8.98	12.95	3.2	3.21	4.42	5.11	6.11	6.22
SrMTT	0.94	1.85	1.38	2.44	1.53	2.7	1.4	1.28	1.74	1.6	1.87	1.72
Casting type	Roundness (%)						Aspect ratio					
	Level 1 (SDAS 37 μm)		Level 2 (SDAS 62 μm)		Level 3 (SDAS 78 μm)		Level 1 (SDAS 37 μm)		Level 2 (SDAS 62 μm)		Level 3 (SDAS 78 μm)	
	Avg.	SD	Avg.	SD	Avg.	SD	Avg.	SD	Avg.	SD	Avg.	SD
NM	45.24	28.42	42.82	28.48	40.8	27.24	2.64	1.37	3.13	1.74	3.3	1.83
SrM	75.24	20.64	77.23	21.45	77.23	21.23	1.81	0.66	1.53	0.37	1.65	0.55
SH	74.76	22.84	74.78	23.2	73.43	23.77	1.85	0.78	1.79	0.75	1.79	0.72
MTT	56.96	27.34	55.26	29.51	51.16	29.97	2.51	1.33	2.91	1.62	2.76	1.52
SrMTT	78.87	20.35	77.32	20.87	75.81	21.48	1.81	0.67	1.83	0.69	1.87	0.72

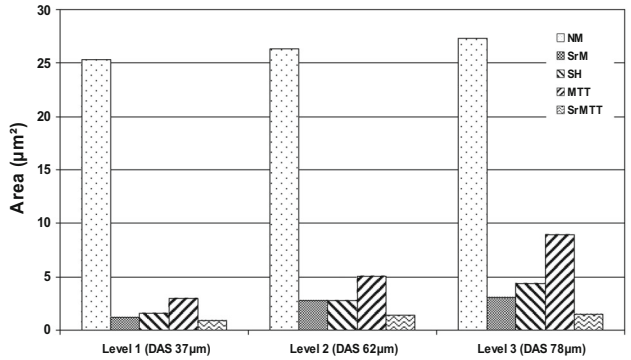

Figure 11. Average Si particle area obtained for as-cast samples taken from different A356.2 alloy castings/levels, showing the effect of (i) solidification rate, casting level/SDAS, and (ii) modification process, casting type.

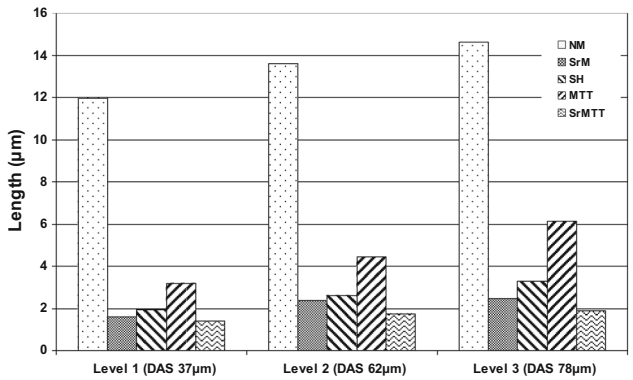

Figure 12. Average Si particle length obtained for as-cast samples taken from different A356.2 alloy castings/levels, showing the effect of (i) solidification rate, casting level/SDAS, and (ii) modification process, casting type.

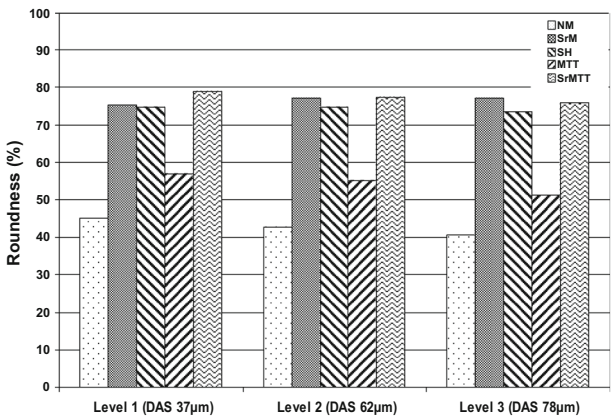

Figure 13. Average Si particle roundness obtained for as-cast samples taken from different A356.2 alloy castings/levels, showing the effect of: (i) solidification rate, casting level/SDAS, and (ii) modification process, casting type.

strength of each casting from one level to another. For instance, at a level measured at 10 mm from the chill end (SDAS of 37 µm), the yield strengths of the NM, SrM, SH,

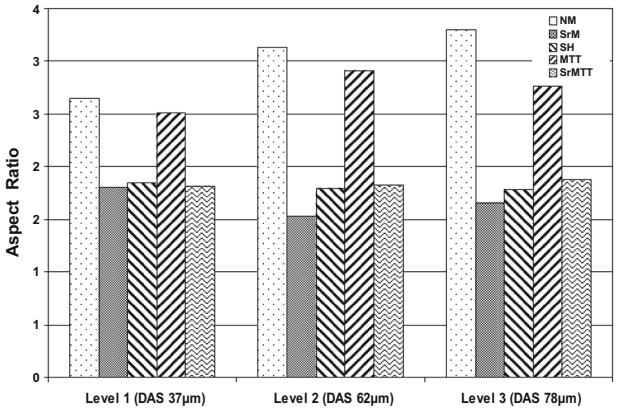

Figure 14. Average Si particle aspect ratio obtained for as-cast samples taken from different A356.2 alloy castings/levels, showing the effect of: (i) solidification rate, casting level/SDAS, and (ii) modification process, casting type.

MTT and SrMTT casting samples are 88, 96, 104, 99 and 94 MPa, respectively. Also, for each casting type, the solidification rate does not appear to affect the yield strength. For example, in the SrMTT casting samples, the yield strengths obtained at the three levels (SDASs of 37, 62 and 78 µm) are 95, 96 and 92 MPa, respectively. The other A356 alloy casting types also display the same tendency.

The UTS values obtained for the various casting types reveal that the SrM, SH and SrMTT processes improve the UTS to a certain extent compared to what occurs in the non-modified (NM) condition, while the MTT-processed casting appears to have no effect, as shown in Figure 16. For instance, at a SDAS of 62 µm, the UTS for NM, SrM, SH, MTT and SrMTT samples is 148, 169, 168, 147 and 158 MPa, respectively. This effect on UTS is related to the improvement observed in the Si particle characteristics, especially with regard to the aspect ratio. In SrM-, SH-, and SrMTT-treated castings, the Si particles are modified from an acicular form to a clearly fibrous morphology, whereas in NM or MTT-treated castings, they still appear as acicular flakes. It should be noted, however, that the improvement is also affected by the solidification rate. As Figure 16 shows, at the high solidification rate (SDAS of 37 µm), improvement in the UTS is marginal, namely 182, 175, 162 and 179 MPa for the SrM-, SH-, MTT- and SrMTT-treated castings, respectively, compared to 180 MPa for the NM casting.

At high solidification rates, the effect of solidification rate, or SDAS, dominates those produced by the other melt treatment/modification processes, as has been recorded for fine dendrite arm spacings, in view of the fact that not only the eutectic silicon but also all of the micro-constituents in the microstructure are refined. The effects of modification take over, however, as the solidification rate decreases, i.e., as the SDAS attains larger values. For example, in the SrM

Table 6. Change in Si Particle Size Achieved for Different Casting Types in Comparison with the Non-modified Casting (NM)

Casting Type	Percentage change in Si particle size					
	% Decrease in area (μm^2)			% Decrease in length (μm)		
	Level 1 (10 mm)	Level 2 (50 mm)	Level 3 (100 mm)	Level 1 (10 mm)	Level 2 (50 mm)	Level 3 (100 mm)
NM	(25.33)	(26.32)	(27.32)	(11.96)	(13.57)	(14.62)
SrM (%)	95.4	89.3	88.7	86.9	82.6	83.1
SH (%)	93.6	89.4	83.9	83.4	80.7	77.5
MTT (%)	88.4	80.9	67.1	73.3	67.5	58.2
SrMTT (%)	96.3	94.7	94.4	88.1	87.2	87.2

Levels 1, 2 and 3 correspond to SDASs of 37, 62 and 78 μm, respectively

Table 7. Change in Si Particle Shape Achieved for Different Casting Types in Comparison with the Non-modified Casting (NM)

Casting Type	Percentage change in Si particle shape					
	% Increase in roundness			% Decrease in aspect ratio		
	Level 1 (10 mm)	Level 2 (50 mm)	Level 3 (100 mm)	Level 1 (10 mm)	Level 2 (50 mm)	Level 3 (100 mm)
NM	(45.24)	(42.82)	(40.80)	(2.64)	(3.13)	(3.30)
SrM (%)	66.31	80.36	89.29	31.44	51.12	50.00
SH (%)	65.25	74.64	79.98	29.92	42.81	45.76
MTT (%)	25.91	29.05	25.39	4.92	7.03	16.36
SrMTT (%)	74.34	80.57	85.81	31.44	41.53	43.33

Levels 1, 2 and 3 correspond to SDASs of 37, 62 and 78 μm, respectively

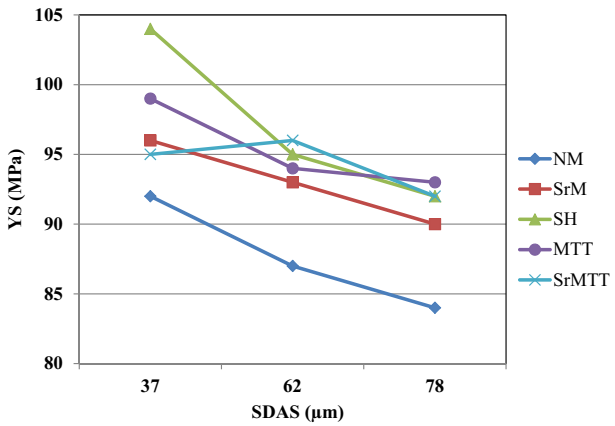

Figure 15. Yield strength of samples in the as-cast condition obtained from different A356.2 casting types.

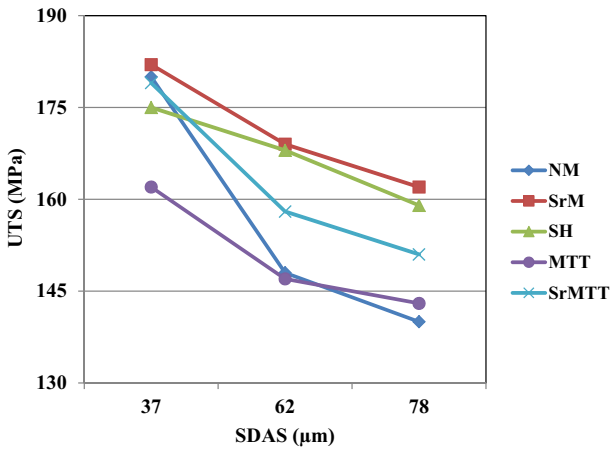

Figure 16. Ultimate tensile strength of samples in the as-cast condition obtained from different A356.2 casting types.

casting, the UTS decreases from 182 to 162 MPa as the SDAS increases from 37 to 78 μm. Similarly, in the case of the SH casting, the UTS is lowered from 175, through 168, to 159 MPa, respectively. This decrease in UTS is related to the increase in the Si particle size and aspect ratio resulting from the decrease in solidification rate. The low UTS value displayed by the MTT casting at 37 μm SDAS was probably the result of the presence of porosity defects and/or inclusions in the gage length portion of the corresponding test bars. Figure 17 shows the results for percentage elongation for the various casting types.

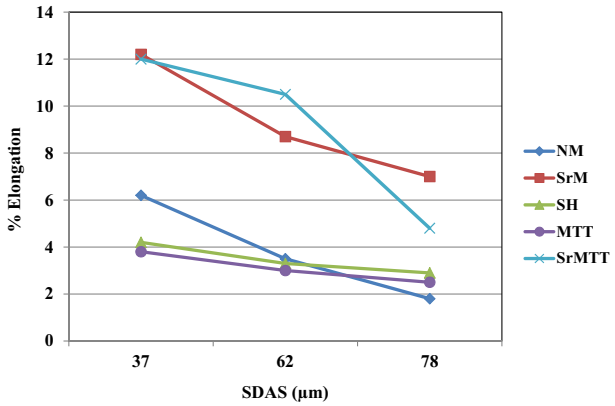

Figure 17. Percentage elongation of samples in the as-cast condition obtained from different A356.2 casting types.

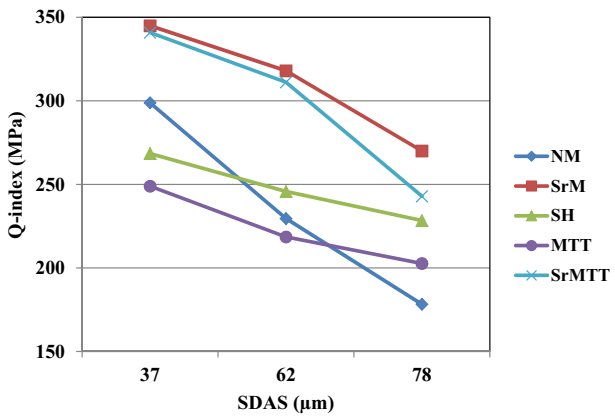

Figure 18. Q-index of samples in the as-cast condition obtained from different A356.2 casting types.

Both SrM and SrMTT processes improve the ductility considerably from ~6 % in the non-modified condition to ~12 %, at 37 µm SDAS. Comparing the plots for the NM and SrM casting samples, the same level of improvement may be obtained with Sr modification, relative to the non-modified case at all solidification rates or SDASs.

Since the SH and MTT processes do indeed refine the Si particles, no significant improvement in ductility may be observed. In fact, the ductility is even lower, by about 2–2.7 %, than that of the NM casting sample, at the high solidification rate, i.e., at a SDAS of 37 µm which may be attributed to the presence of oxide films.[19–21] The ductility decreases fairly gradually with an increase in secondary dendrite arm spacing, from ~4 % at 37 µm SDAS to ~3 % at 78 µm SDAS. Compared to the NM casting sample, the longer solidification time in the case of the SH casting sample would provide more time for distributing the Si particles homogeneously in the casting and result in improving the ductility (cf. ~3 % with ~1.5 % for NM). To summarize, the ductility of A356 alloys subjected to different melt treatment/modification processes is determined by the dendrite arm spacing, the eutectic Si particle size and aspect ratio, as well as by the presence of casting defects and other microconstituents such as hard intermetallic phases.[22] The observations for the MTT-processed casting are in keeping with those of Wang.[17]

The quality index, Q, was introduced by Drouzy et al.[18] as a means to better interpret tensile test data. Rather than using ductility directly, they defined, instead, the quality index Q, in terms of the ultimate tensile strength and percent elongation (El > 1 %) and a coefficient k, having a value of 150 MPa for the Al–7Si G06 alloy studied by them. This alloy is equivalent in composition to A357 alloy without beryllium.

In view of the tensile properties of the different A356.2 alloy casting studied in the present work, it would be interesting to see how the different factors, for example, cooling rate, modification process and superheat, would affect the 'quality' of the alloy or casting, in terms of the quality index.

Accordingly, the Q values for the various samples were calculated based on the equation:

$$\text{Quality index} = \text{UTS(MPa)} + 150\log(\text{EL}\%)$$

with Q expressed in MPa units.

The results are plotted in Figure 18 for the various A356.2 alloy casting types, at each of the three SDAS levels. As can be seen, a much more consistent behavior is observed when the quality index is used as an indicator of the tensile properties than the individual properties themselves.[6] Obviously, the finer microstructures at the 37 µm SDAS level display superior quality. From the application point of view, a compromise is often sought between the strength and ductility requirements of a casting prepared for a specific application. The Q plots of Figure 18 are a very convenient means to determine this. As can be seen, the Sr and SrMTT castings display the best 'quality' overall, among all the casting types. The lower 'quality' of the SH and MTT castings would probably be attributed to particle clustering effects and inhomogeneous distribution of the Si particles in their microstructures.

Figure 19 shows some examples of the fracture surface of samples cast under different conditions (level #1). Coarse acicular eutectic Si particles are the main feature in non-treated alloys (coded NM) as displayed in Figure 19a. Application of the MTT process (no Sr was added) resulted in a significant reduction in the length of the acicular Si particles without noticeable change in the Si morphology (Figure 19b). The white arrows in Figures 19a, b reveal the presences of cracks within the Si particles. Some of these black cracks could be as well due to the presences of bifilms.[19–21]

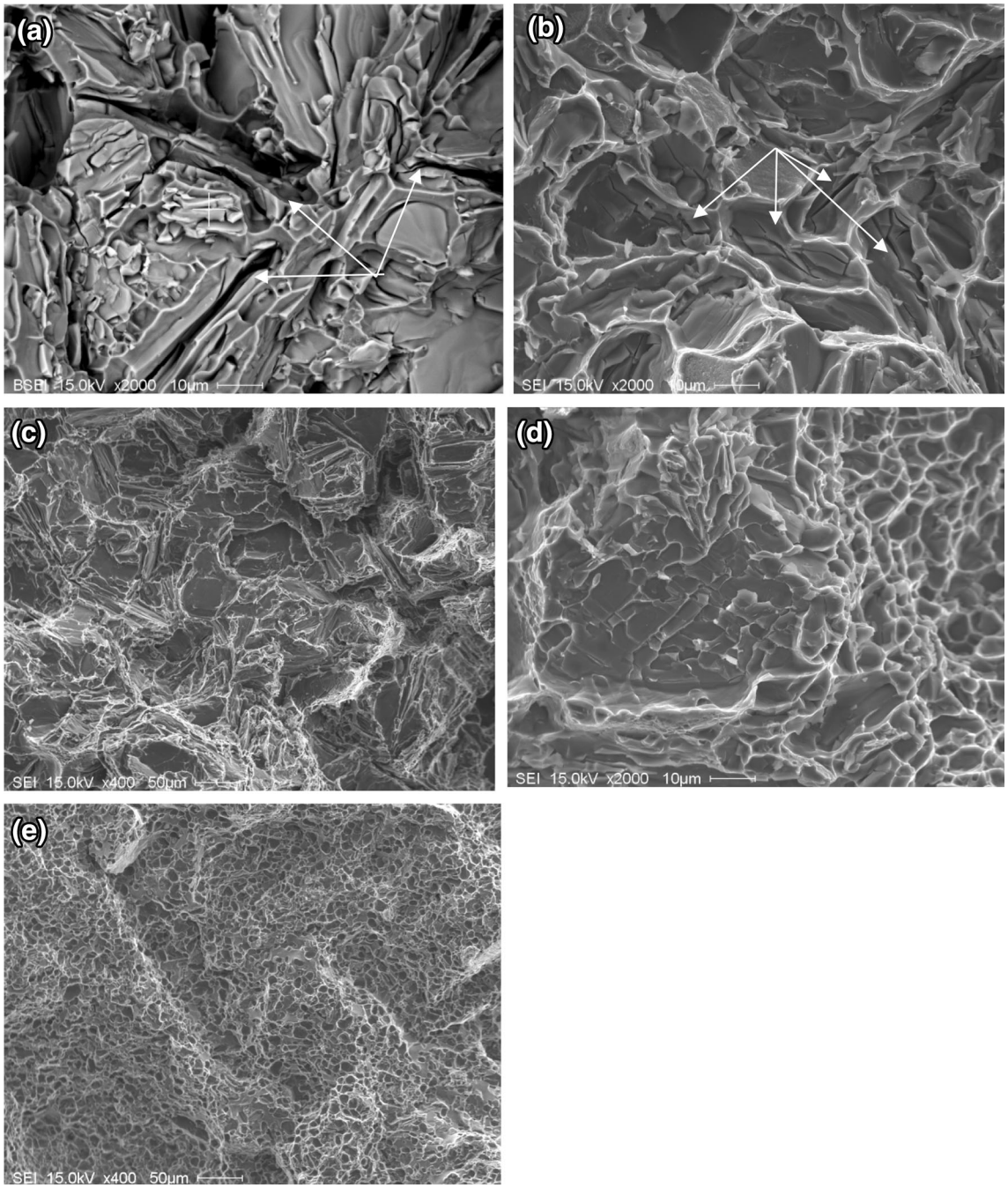

Figure 19. Fracture surface of samples cast under different conditions (corresponding to level #1): (a) NM, (b) MTT, (c) SH, (d) high magnification of (c), (e) SrMTT. Note the cracks within the Si particles in (a) and (b)—white arrows.

Although SH alloy does not contain Sr, however, due to high pouring temperature (900 °C) and hence the increase in solidification time, the Si particles retained their acicularity to some extent as exhibited in Figure 19c. Figure 19d shows the development of dimple structure over certain regions. Figure 19e reveals a well defined dimple structure when the alloy was modified with approximately 100 ppm Sr coupled with MTT treatment (pouring temperature was about 750 °C) corresponding to the best tensile properties illustrated in Figures 15, 16, 17.

Conclusions

1. The acicular eutectic silicon observed in non-modified A356.2 alloy can be modified using various means such as Sr modification (SrM), superheat melt (SH), melt thermal treatment (MTT) and a combination of Sr modification and MTT (SrMTT).
2. Strontium modification, superheat and Sr-modified-MTT-processed castings provide fine eutectic

Si particles, the SrM and SrMTT processes giving the best modification results. The MTT process alone provides a moderate amount of modification.

3. Compared to all casting types, the SrMTT casting shows the best results in that not only the Si particle sizes are the smallest among all the castings, but these values remain approximately constant over the ranges of solidification rates studied. This has great significance from an application point of view, as cast parts often contain sections of ranging thickness, and the use of a SrMTT-processed Al–Si alloy melt would ensure a relatively uniform eutectic Si particle size throughout the casting and, hence, guarantee its overall properties.
4. Both size and morphology of the eutectic silicon particles are affected by the modification process used. The SrM, SH and SrMTT castings show well-modified fibrous Si particles, whereas the MTT casting exhibits Si particles that, although refined to a certain extent, still retain their acicular morphology.
5. Solidification rate affects the eutectic Si particle size in that a higher solidification rate produces finer Si particles. However, within the range of solidification rates provided by the end-chill mold used in this work, the solidification rate does not affect the morphology of the Si particles.
6. An analysis of the tensile test data for the various A356.2 alloy casting types (NM, SRM, SH MTT and SrMTT) in the as-cast condition shows that neither solidification rate nor melt treatment/modification process has any influence on the yield strength.
7. Tensile strength can be improved by SrM, SH and SrMTT treatments, while the MTT process has no apparent influence on UTS.
8. Both SrM and SrMTT treatments can greatly improve the ductility of A356 alloy castings, whereas SH and MTT processes do not show any significant improvement. Higher percentage elongations can be achieved with higher solidification rates.

Acknowledgments

The authors would like to thank Dr. Ehab Samuel of the National Research Council Canada—Aluminium Technology Centre for editing the present research article.

REFERENCES

1. D. Apelian, S. Shivkumar, G. Sigworth, Fundamental aspects of heat treatment of Cast Al–Si–Mg alloys. AFS Trans. **97**, 727–742 (1989)
2. S. Shivkumar, C. Keller, D. Apelian, Aging behavior in cast Al–Si–Mg alloys. AFS Trans. **98**, 905–911 (1990)
3. J.R. Davis (ed.), *Aluminum and aluminum alloys* (ASM International, Ohio, 1993), p. 627
4. S. Shankar, Y.W. Riddle, M.M. Makhlouf, Nucleation mechanism of the eutectic phases in aluminum–silicon hypoeutectic alloys. Acta Mater. **52**, 4447–4460 (2004)
5. J.E. Gruzleski, The art and science of modification: 25 years of progress, Silver Anniversary Paper. AFS Trans. **100**, 673–683 (1992)
6. W. Jie, Z. Chen, W. Reif, K. Muller, Superheat treatment of Al–7Si–0.55Mg melt and its influences on the solidification structures and the mechanical properties. Metall. Mater. Trans. A **34A**, 799–806 (2003)
7. B. Tolui, A. Hellawell, Phase separation and undersolidification in an Al–Si eutecticalloy—The influence of freezing rate and temperature gradient. Acta Metall. **24**, 565–573 (1976)
8. L.M. Hogan, H. Song, Interparticle spacings and undersolidifications in Al–Si eutectic microstructures. Metall. Trans. A **18A**, 235–237 (1970)
9. M.F. Ibrahim, E.M. Elgallad, S. Valtierra, H.W. Doty, F.H. Samuel, Metallurgical parameters controlling the eutectic silicon charateristics in be-treated Al–Si–Mg alloys. Mater. **9**(2), 1–17 (2016)
10. P.E. Crosley, L.F. Mondolfo, The modification of aluminum-silicon alloys. AFS Trans. **74**, 53–64 (1966)
11. P.S. Popel, V.E. Sidorov, Microheterogeneity of liquid metallic solutions and its influence on the structure and properties of rapidly quenched alloys. Mater. Sci. Eng. A **226–228**, 237–244 (1997)
12. S. Eguskiza, A. Niklas, A.I. Fernández-Calvo, F. Santos, M. Djurdjevic, Study of strontium fading in Al–Si–Mg and Al–Si–Mg–Cu alloy by thermal analysis. Int. J. Metalcasting, 45–50 (2015)
13. J. Wang, S. He, B. Sun, Y. Zhou, Q. Guo, M. Nishio, A356 alloy refined by melt thermal treatment. Int. J. Cast Met. Res. **14**, 165–168 (2001)
14. R. Lazarova-Mancheva, R. Kovacheva, G. Bachvarov, V. Manolov, Influence of the Solidification rate on the geometric parameters of eutectic silicon in AlSi7Mg castings. Prakische Metallographie **39**, 28–35 (2002)
15. F. Paray, J.E. Gruzleski, Microstructure-mechanical property relationships in a 356 alloy. Part I: Microstructure. Cast Metals **7**, 29–40 (1994)
16. S. Shivkumar, S. Ricci Jr., C. Keller, D. Apelian, Effect of solution treatment parameters on tensile properties of cast aluminum alloys. J. Heat. Treat. **8**, 63–70 (1990)
17. J. Wang, S. He, B. Sun, K. Li, D. Shu, Y. Zhou, Effects of melt thermal treatment on hypoeutectic Al–Si alloys. Mater. Sci. Eng. **A338**, 101–107 (2002)
18. M. Drouzy, S. Jacob, M. Richard, Interpretation of tensile results by means of quality index and probable yield strength. AFS Int. Cast Metals J. **5**, 43–50 (1980)
19. X. Cao, J. Campbell, Oxide inclusions defects in Al–Si–Mg cast alloys. Can. Metall. Q. **44**, 435–448 (2005)

20. J. Campbell, An overview of the effect of bifilms on the microstructure and properties of cast alloys. Metall. Mater. Trans. B **37B**, 857–863 (2006)
21. Z. Ma, A.M. Samuel, F.H. Samuel, H.W. Doty, S. Valtierra, A study of tensile properties in Al–Si–Cu and Al–Si–Mg alloys: effect of β-iron intermetallics and porosity. Mater. Sci. Eng. A **490**(1–2), 36–51 (2008)
22. E. Samuel, A.M. Samuel, H.W. Doty, S. Valtierra, F.H. Samuel, Intermetallic phases in Al–Si based cast alloys: new perspective. Int. J. Cast Met. Res. **27**, 107–114 (2014)